

Repair Concepts for Advanced Composite Structures

S. H. Myhre*

Northrop Corporation, Hawthorne, Calif.

and

C. E. Beck†

Air Force Flight Dynamics Laboratory, Wright Patterson AFB, Ohio

Single scarf joints of a vacuum cocured graphite/epoxy laminate bonded to an autoclave precured laminate have been fabricated and subjected to an extensive series of structural tests under the following conditions: dry and wet, tension and compression, cold and hot, static and post-fatigue. Several adaptations of this joint to other situations were fabricated and tested under selected conditions. An external patch repair was also developed and tested extensively. Both the scarf joint and the external patch were later used to repair 4-in. diam holes in flat panels. The size of the damaged area to which either approach is applicable appears to be unlimited. All results are very encouraging as to the feasibility of successful repairs in graphite/epoxy laminates.

Introduction

THE reparability of advanced composite structures has been considerably advanced in the past two years. Though new techniques will continually be devised for special situations, the basic question has been resolved: graphite/epoxy is a repairable structural material.

Figure 1 expresses the two aspects of reparability which drive toward high-strength restoration and low cost. Of course, aircraft downtime and performance degradation should be evaluated and included in cost considerations. Strength restoration of 80% of the tension ultimate allowable (F_{tu}) is generally considered sufficient to cover all but the most unusual cases. The compression ultimate allowable (F_{cu}) may be higher than tension but it is rarely used as the critical design allowable except where F_{cu} is degraded, as in the case of the hot-wet environment.

Earlier efforts to repair advanced composite materials have generally resorted to an external patch concept. Alternate layers of titanium foil and film adhesive making a concentric stepped patch have been used.¹ Such a repair may be adequate in a particular case, but it suffers from the high shear and peel stresses at the edge of the hole. The external protrusion increases, and the joint efficiency decreases as the thickness of the laminate and the area of the repair become larger.

By contrast, the scarf seems particularly well adapted to advanced composite materials as it was to wood, the original composite material. However, attempts to utilize this approach had not met with outstanding success. A boron/epoxy 27-ply multidirectional laminate joined to an equal thickness (0.135 in.) of 6A1-4V-titanium alloy through a 3 deg scarf with MB 329 adhesive, developed an ultimate load of about 54% of the laminate allowable strength.² One would like to

see a repair joint develop 80% or more of the laminate allowable to be better suited for permanent repair of primary composite aircraft components.

These meager results were not encouraging, nor were our own early attempts at Northrop. Yet the scarf joint with a cocured patch essentially flush with the outer mold line (OML) looked promising if it could be understood and optimized. With this basic concept, Northrop approached the Large Area Composite Structure Repair (LACOSR) program.^{3,4} The Air Force funded the program to answer in a systematic way the question of what constitutes a safe, reliable and operationally suitable repair for large area damage to composite structure. "Large area" is defined as essentially unlimited in so far as applicability of the repair techniques is concerned. The program has evaluated the environmental effects of oil, fuel, paint stripper, and absorbed moisture; the service conditions of tension and compression loads, of prior fatigue history and service temperature; processing variables such as vacuum bag curing vs autoclave curing, shop machining vs portable equipment dressing of the damaged area and precured vs cocured adherends; and finally, a group of inherent features including the laminate material thickness, stacking order, the structural form, accessibility, and protrusion limitations.

Basic Considerations

Closed Options

Consider first those inherent features of a repair which are closed options to a repair team and which were determined somewhat arbitrarily for the LACOSR program. All parent laminates discussed here were made from AS/3501-5

Presented as Paper 78-479 at the AIAA/ASME 19th Structures, Structural Dynamics and Materials Conference, Bethesda, Md., April 3-5, 1978; submitted June 2, 1978; revision received Dec. 14, 1978. Copyright © American Institute of Aeronautics and Astronautics, Inc., 1978. All rights reserved. Reprints of this article may be ordered from AIAA Special Publications, 1290 Avenue of the Americas, New York, N.Y. 10019. Order by Article No. at top of page. Member price \$2.00 each, nonmember, \$3.00 each. Remittance must accompany order.

Index categories: Structural Design, Reliability, Maintainability and Logistics Support; Structural Composite Materials.

*Engineering Specialist, Advanced Structural Concepts Department, Member AIAA.

†Project Engineer, Structures Division.

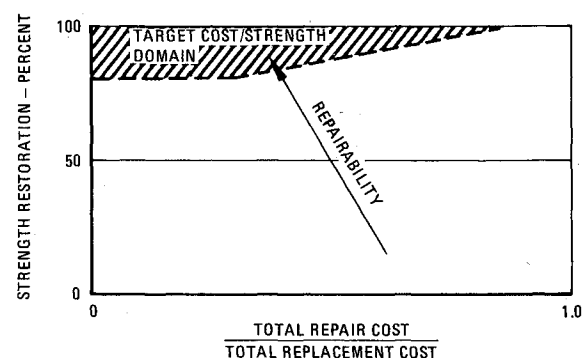


Fig. 1 Repairability.

Table 1 AS/3501-5 graphite/epoxy 16-ply parent-laminate allowables^a

Temp, °F	Tension Allowable		Compression Allowable	
	Loading, lb/in.	Strain, μin./in.	Loading, lb/in.	Strain, μin./in.
-65	6210	—	9740	—
RT	6860	11,000	7600	12,000
265	5750	—	4710	—

^aCured at 100 psi/350°F/2 h; laminate stacking $[(\pm 45/0/90)_2]_s$; water content = 1.0%; "B" basis tension allowables from Ref. 5 are 90% of average of 20 tests; compression allowables are 80% of average of 3 tests.

graphite/epoxy tape. A 16-ply graphite laminate $[(0/\pm 45/90)_2]_s$ was chosen as representative of a large class of laminates which carry both normal loads and shear. The number of plies was doubled or reduced by half in some cases, and the stacking order was later changed so that this generic laminate was considered from many angles. The ultimate tension and compression fiber-failure allowables are given in Table 1. Minimum damage size is defined as a 4-in. diam hole completely through the panel.

Two structural forms were considered: a flat laminate panel and a flat honeycomb sandwich panel. Eight-ply laminates $(\pm 45/0/90)_s$ were used on the faces so that the sandwich represents relatively lightly loaded structure. While curved panels were not repaired, the need to face the problems of curvature were not ignored. The approach developed here is quite applicable to curved panels and shapes.

The operational environment and load conditions imposed on the repair-joint concepts range from -65°F to 265°F temperature, tension and compression, dry and wet, static and post-fatigue. "Dry" refers to the repair assembly. All of the parent laminates were soaked in 180°F deionized water until the laminate had absorbed 1% moisture by weight. "Wet" repairs were subsequently moisture conditioned at 180°F and 95% relative humidity for 30 days. The post-

fatigue test is a determination of residual strength after a two-lifetime history of fatigue loading using the load spectrum developed for the F-5F lower inboard wing skin. The exceedance curve, shown in Fig. 2, represents 1000 hours of flying with compressive loads deleted. Three specimens of a given repair were run with the maximum fatigue load at 41.5% of parent laminate allowable and another three at a maximum fatigue load of 22.9% of parent allowable. The residual strength reported here is the minimum of these two results.

Design Options

With the repair job thus defined, what are the options open to us? It may be well to grow an option tree such as shown in Fig. 3. Our first choice was the bonded branch, based on the proposition that the graphite/epoxy is inherently a bonded structure and bonding to it is really not difficult.

The patch material chosen was AS/3501-6 graphite/epoxy cured at 15 psi vacuum bag pressure, and 350°F (heated at 3°F/min) for two hours and cooled to 150°F before release of vacuum pressure. Tensile strength of the patch laminate is about 84% of the parent allowable because the patch is vacuum cured. The patch arrangement is generally the same as the parent laminate with the addition of a few plies as necessary in the primary loading directions. Cocured patches were used to eliminate close tolerance-fit problems in the scarf joint.

The adhesive FM-400 (0.07 psf film) was selected to meet the 265°F service temperature requirement. Rail shear tests on a seven-ply laminate of the adhesive cured at 15 psi, 350°F, 1 h resulted in room temperature shear strengths of 6640 psi dry, and 4240 psi wet (immersed in 180°F water for seven days). Meaningful shear properties are most difficult to obtain. The cure conditions, adhesive thickness, moisture content, and test methods all influence the results. Sophistication of the analysis to which the data is to be applied also dictate the properties and the strength values to be used. In the end, pragmatism prevails.

Repair Concepts

The five repair-joint concepts shown in Fig. 4 were developed for the generic laminate repair. Each of these will be discussed in detail.

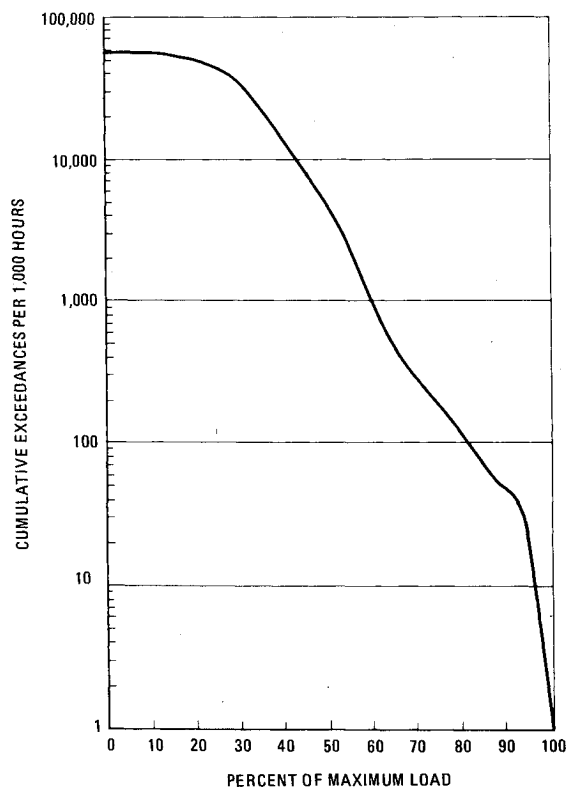


Fig. 2 F-5E load spectrum for wing lower skin at BP 29.5.

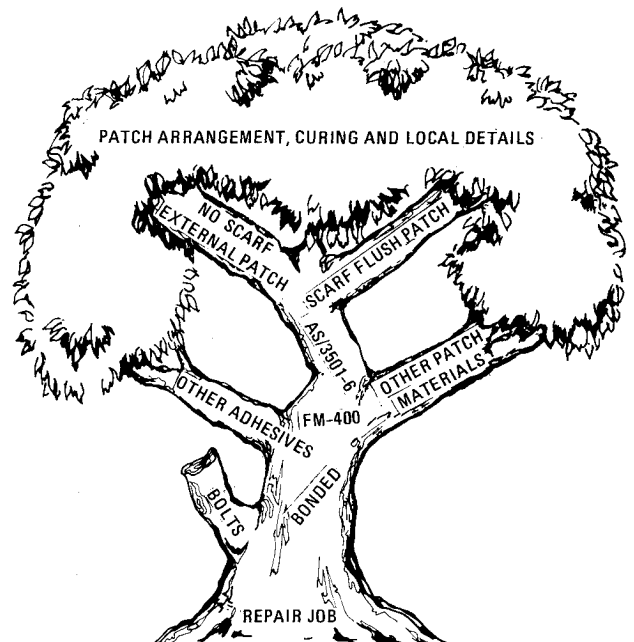


Fig. 3 Repair design option tree.

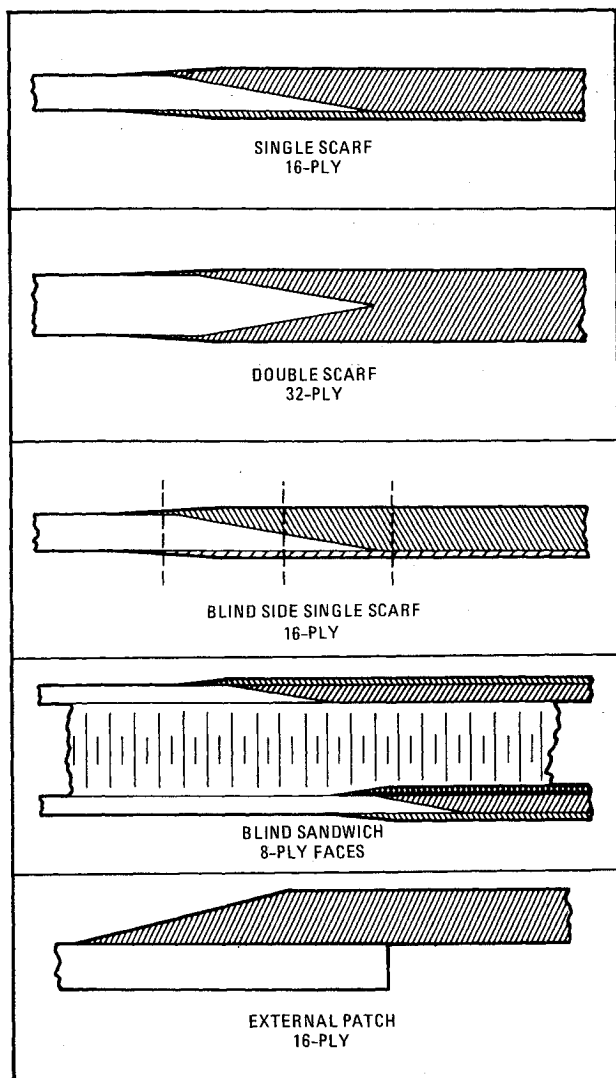


Fig. 4 Repair-joint concepts.

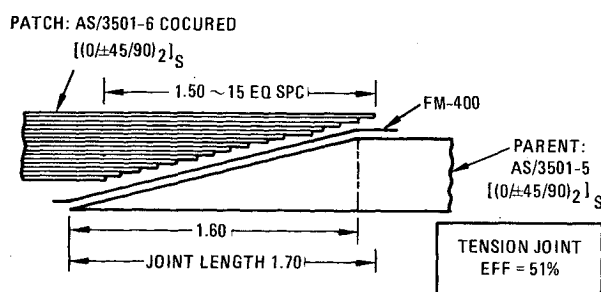


Fig. 5 Basic cocured 16-ply scarf-joint design.

Bonded Scarf-Joint Flush Repair

A cocured scarf joint in graphite/epoxy composite material has been developed, capable of restoring nearly the full parent allowable strength. Several preliminary tests were made to verify specific points indicated by the analysis as described in the Appendix.

The first point concerned the scarf taper ratio: length/thickness. Increasing the taper ratio will improve the strength but not in proportion to the increase in length. A taper of 0.10 in. per ply (18/1) was selected, though this is much lower than has been commonly thought necessary for wood or advanced composites. Joining the 16-ply generic parent laminate to a 16-ply patch with the same

PLY END CUT	TENSION ULTIMATE STRENGTH (LB/IN)	MODE OF FAILURE	% OF PARENT ALLOWABLE
CONTROL	5260	PEEL	77
0.10	6633	TENSION	97
0.20	7063	TENSION	103
0.40	6900	TENSION	100
0.125			

Fig. 6 Results of ply termination tests.

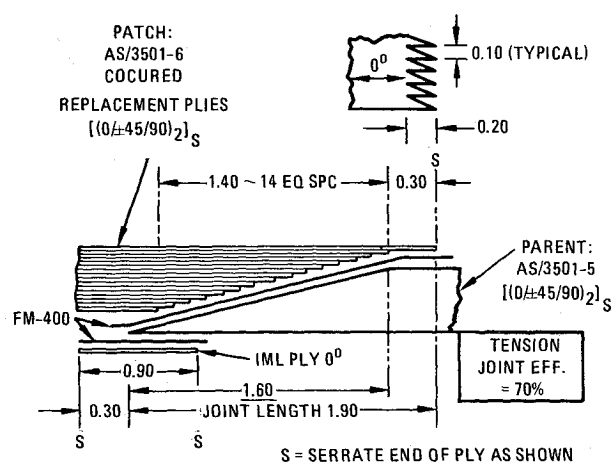


Fig. 7 Refined scarf-joint design, including serrations.

$[(0/\pm 45/90)_2]_s$ stacking order as shown in Fig. 5 resulted in shear failure in the joint at 51% joint efficiency.

The second point concerned the ends of the longest 0-deg patch ply. What could be done about the high shear stress and peeling action known to exist at the end of the ply? Special ply termination tests were run on the 16-ply generic parent laminate with a 0-deg ply bonded to each surface on each end but terminating near the center of the specimen. Tension load was applied. The control specimen with the terminating plies cut off straight and perpendicular to the longitudinal axis failed at 77% of the parent allowable by peeling the extra ply away. Of specimens with several kinds of serrations cut into the end of the terminating plies, as shown in Fig. 6, all failed near 100% of the parent allowable and failed in laminate tension. No peeling occurred on any of nine specimens having a total of 36 serrated ply ends. A pair of commercial pinking shears cuts a satisfactory serration 1/8-in. deep.

The third point concerned the end of the parent laminate. Shop people must be instructed to scarf the laminate all the way to the inner surface. The edge may look a bit ragged and they are inclined to trim it off. However, if this inner surface ply is a 0-deg ply (i.e., aligned with the load) this ply needs to be scarfed more than the others. In order that this inner surface 0-deg ply should be unloaded through two surfaces rather than one, a small serrated patch ply was applied as shown in Fig. 7. The outer surface patch ply was also extended slightly and serrated as shown. By adding this small amount of material and serrating the ply ends, the joint efficiency was raised to 70% and the mode of failure changed to patch-laminate tension.

Having resolved the details of the splice, the repair itself can now be considered. The generic parent laminate is

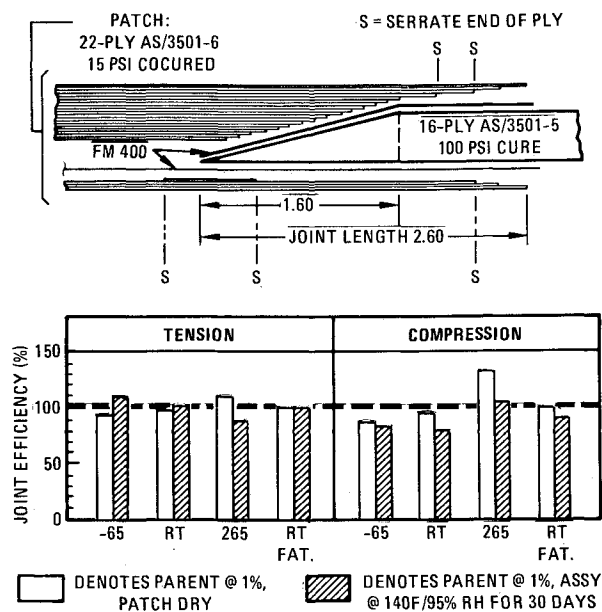


Fig. 8 Final single-scarf flush repair.

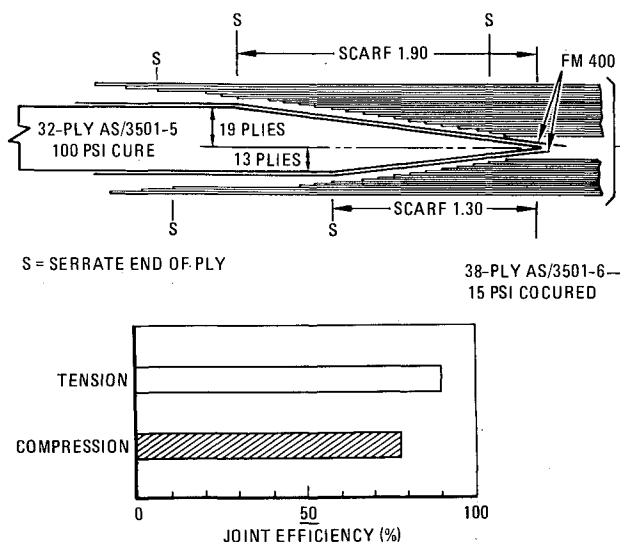


Fig. 9 Double-scarf flush repair.

assumed to be loaded in shear as well as longitudinal tension and compression. Therefore, one ply was added in each of three directions (0, +45 and -45) on both sides of the laminate as shown in Fig. 8. This joint developed 97% joint efficiency (RT dry tension) and consistently failed in parent-laminate tension. This is a very satisfactory repair concept.

An earlier version involved essentially the same splice but did not continue the six added plies to the end of the specimen. These failed in repair-laminate tension with joint efficiencies of 83% at room temperature dry, 80% at -65°F dry, and 87% at room temperature dry with prior fatigue history. Tests on these latter conditions were not repeated with the improved design. Rather, the results obtained were scaled by the ratio of 97/83 making an estimated joint efficiency of 93% at -65°F and 101% with prior fatigue history as shown in Fig. 8. The same specimen was tested at 265°F where failures were parent-laminate tension at 110% of the 265°F tension allowable.

The stacking order of the generic parent laminate was changed to $[(\pm 45/0/90)_2]_s$ because this was thought to be more typical of evolving aircraft practice. The patch was changed accordingly to keep the replacement plies in the same

order, but otherwise the repair remained essentially unchanged from the design of Fig. 8. The test results, completed with this stacking order, are shown in Fig. 8 for tension and compression, dry and wet, -65°F, RT and 265°F, static and post-fatigue residual strength testing. Apparently, neither moisture, cold and hot temperatures, nor prior fatigue history significantly degrade the structural efficiency of the single scarf joint.

Double Scarf-Joint Flush Repair

The double scarf joint permits a shorter joint length and less parent material removed than a single scarf. Using the same 18/1 taper ratio, the design for a 32-ply generic laminate repair was patterned after the single scarf joint. Three plies ($\pm 45/0$) were added on both surfaces and the two longest 0-deg plies on either side were serrated. Tension and compression specimens and the results of room temperature dry tests are shown in Fig. 9. The results are satisfactory to demonstrate the validity of this approach though additional patch material appears required for full strength restoration.

Blind-Side Bonded Scarf Repair

The difficulties involved in repairing a panel with access from one side only are obvious; the solutions are not. The substantial improvement (37%) achieved by even a small patch bonded to the inside surface (Fig. 7 cf. Fig. 5) could not be ignored. The design presented here evolved out of numerous considerations, not the least of which were: 1) how to locate the inside patch, and 2) how to effect a good bond.

A precured AS/3501-6 laminate ($\pm 45/0$)_s was chosen for the inside patch for the following reasons: 1) no new bonding materials or logistics are involved, 2) tapering the patch is made easy by cutting the plies to the proper size and serrating the edge where necessary, and 3) forming the patch to a compound curvature, if necessary, can be done without expensive tools, using the outer surface of the part to make a mold. The laminate stacking order is symmetric and continues to be so even as internal plies are terminated.

Locating the internal patch could require some ingenuity. With access limited to only the external surface, the patch must be installed through the damage cutout. A long narrow hole offers the easy solution of rotating the panel into place; however, through a circular hole, bending the thin panel to insert it could be considered. The six-ply panel can be elastically bent to a 2-in. radius of curvature without damage. Once in place, the panel is held against the blind-side (inner) surface of the panel while holes are drilled through both pieces from the outside and Clecos are installed.

The splice detail in Fig. 10 shows the blind-side panel bonded to the inner surface. The drill template remained in place during this bonding cycle to provide support to the Clecos beyond the edge of the parent laminate and through the scarfed area. The holes must be filled after removal of the Clecos to prevent vacuum leaks during the secondary cocuring of the flush patch. The cocured part of the repair, consisting of ($\pm 45/0$) plies plus replacement plies, is bonded in the second cure with vacuum pressure, bagged on the outside surface only.

Results of the blind-side repair tests at various temperatures, moisture, and load conditions are given in Fig. 10. The lowest joint efficiency shown is 84% and, in general, the results indicate that the blind-side repair can be made every bit as good as one with access to both sides if the blind-side patch can be adequately bonded via techniques like those demonstrated here.

Blind-Side Sandwich Repair

The approach to honeycomb sandwich repair taken here is a scarf joint on both inner and outer eight-ply faces as shown in Fig. 11. The inner face is repaired first, following much the same procedure as used for a blind-side monolithic laminate

tested. Multiple failure modes were common, indicating that the repair is well matched to the parent-laminate capability, where failures generally occurred.

Bonded External Patch Repair

The no-scarf external patch option offers some advantage of simplicity. The damaged area is removed, leaving a straight hole. A graphite patch is precured to a surface representing the outer moldline, then bonded to the damaged surface. Such a patch, being eccentric to the skin, must be designed for the bending induced by this eccentricity. The bending strains are surprisingly high. Additional plies required for the bending increase the eccentricity, but the problem does converge.

The real problem is the peeling and high shear stress on the bondline at the edge of the hole. The peeling problem was attacked empirically since it is not amenable to analysis. Six configurations were investigated, five of which involved some simple treatment at the edge of the hole. Three configurations and the test results are given in Fig. 12. Small blind rivets at 1.0-in. spacing make a significant improvement by resisting the peel force. The glass fabric and FM-400 adhesive filling the undercut make another improvement by relieving the shear stress peak. Observing the specimen as load is increased reveals no indication that the rivets resist shear until after the bond has failed.

To stabilize the specimen for compression loading, the repaired laminate was assembled into a honeycomb sandwich beam. This specimen form was then used for all subsequent tests in tension as well as compression. The beam assembly prevents local rotation of the laminate and the resulting peeling. This raised the joint efficiency from 78% to 93% for room temperature dry tension. Complete results of these four-point beam tests of the external patch repair are shown in Fig. 13. With the change in specimen form, the mode and location

of failure also changed from peeling at the edge of the parent laminate to a failure at the edge of the patch. Special treatment was also given at the edge of the patch by increasing the step length and serrating the end of the first three 0-deg plies. Having these three 0-deg plies on the surface appears now to be detrimental to the repair in this area. The compression failures appeared consistently at the end of the second longest ply of the patch. The effect of the longest ply joggling over the end of the second longest ply will be seen more dramatically in the larger panels to be discussed below.

Repairs of Panels With 4-In. Diameter Holes

With the validation of several repair-joint concepts via the uniaxial testing just discussed, it remains to substantiate the extension of these concepts, to three-dimensional, real world applications. To some extent, this was accomplished for the scarf-joint flush repair and the external patch repair using the 16-ply 12-in. \times 48-in. panels of Fig. 14. Each panel was loaded as a four-point beam. Both repairs are direct applications of the joints previously evaluated.

Four panels with the scarf-joint flush repair were constructed, three being scarfed with preliminary router cuts and finished with a sanding disk as shown in Fig. 15. The fourth was prepared with a milling machine with the intent of determining the sensitivity of repair strength to the method of making the scarf. This panel and two others were loaded with the repair in tension, resulting in 109% joint efficiency. All failed in parent-laminate tension as shown in Fig. 16. No improvement was gained by the milling machine scarfing. The one panel tested with the scarf repair in compression achieved 92% of the parent-laminate ultimate compression allowable, failing in patch compression and peel. No indication of early incipient failure was evident in any of the scarf-joint flush repairs. These results are presented in Fig. 17 in comparison with results from the panels repaired with an external patch.

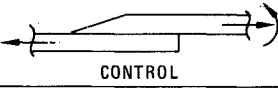
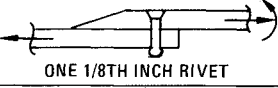

FM-400 BONDED JOINTS (WIDTH = 1.00 INCH)	FAILURE MODE	JOINT EFF
 CONTROL	PEEL AND SHEAR FAILURE	0.52
 ONE 1/8TH INCH RIVET	SHEAR AND PATCH NET TENSION FAILURE	0.73
 ONE RIVET & GLASS FABRIC	SHEAR AND RIVET HEAD PULL-THRU FAILURE	0.78

Fig. 12 External patch concepts.

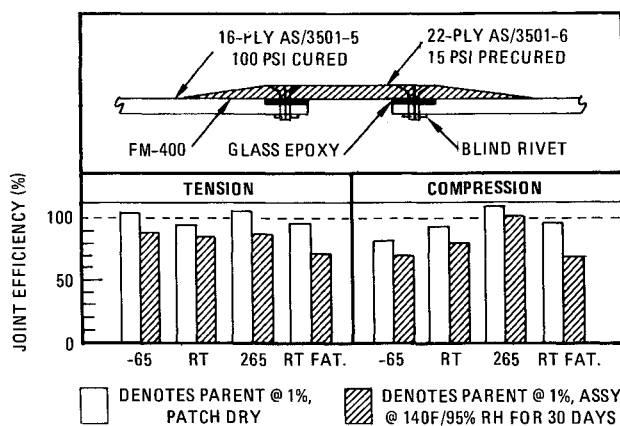


Fig. 13 External patch joint.

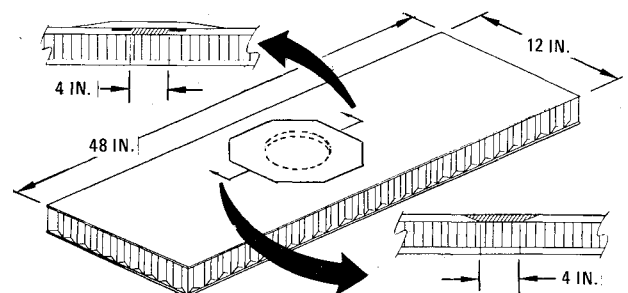


Fig. 14 Holed panel repairs.

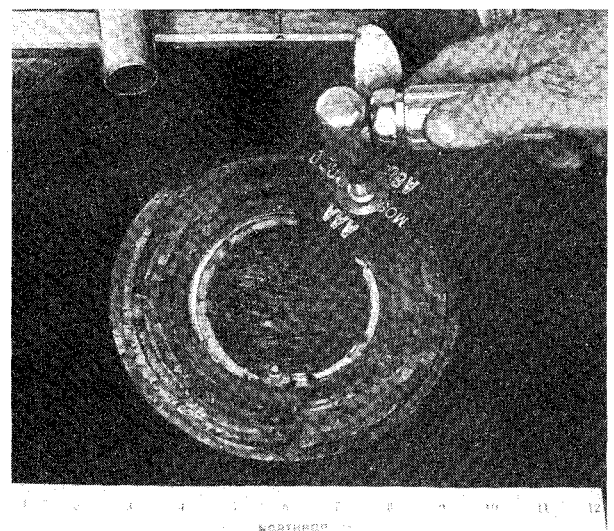


Fig. 15 Scarfing the 4-in. diam hole.

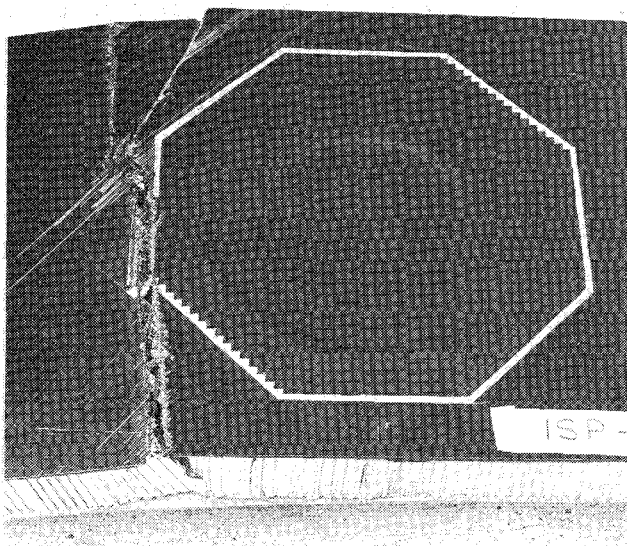


Fig. 16 Typical tension failure of scarf-joint repair panel.

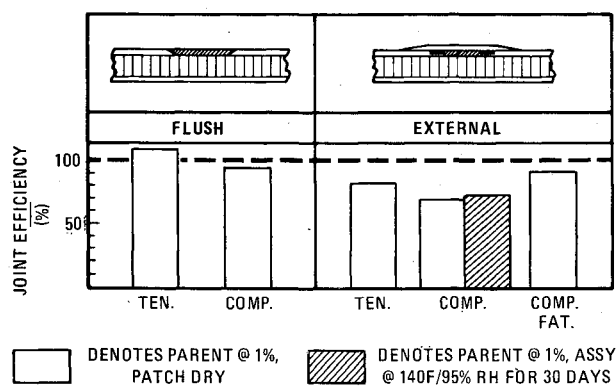


Fig. 17 Holed panel results.

Ten panels, each with a 4-in. diam hole were repaired with an external patch designed for longitudinal loading only. The results shown in Fig. 17 are seen to be lower than the corresponding results on the scarf-joint flush repair and are also considerably lower than the corresponding results on 1-in. wide beams. No sign of incipient failure was evident in any of the tension panels. However, those panels with the repair in compression showed considerable incipient failure beginning at 25% of the parent ultimate compression allowable. Figure 18 shows incipient failure at 35% of the parent allowable. Failure begins where the surface ply (0-deg) joggles over the next longest ply. While this joggle is only a 0.0055-in. step, it is nevertheless seen to have had a significant effect on the ability of the ply to resist failure. Once a local failure occurs, it grows and is joined by others as load is increased, until the entire patch is peeled off. Concern over fatigue loading would appear justified where the maximum compression loads would be high enough to cause such incipient failure. However, spectrum compression fatigue loading to a maximum of 37% of the parent compression allowable resulted in no incipient failure. After fatigue loading, incipient failure began during residual strength testing at 45% of the parent compression allowable. It appears that a stress-relieving mechanism takes place under fatigue loads which suppresses the incipient failure.

Remaining Work and Conclusions

The remaining tasks of the LACOSR program include a series of tests on a partially damaged 50-ply graphite laminate and a 64-ply hybrid laminate. A box beam, large enough for

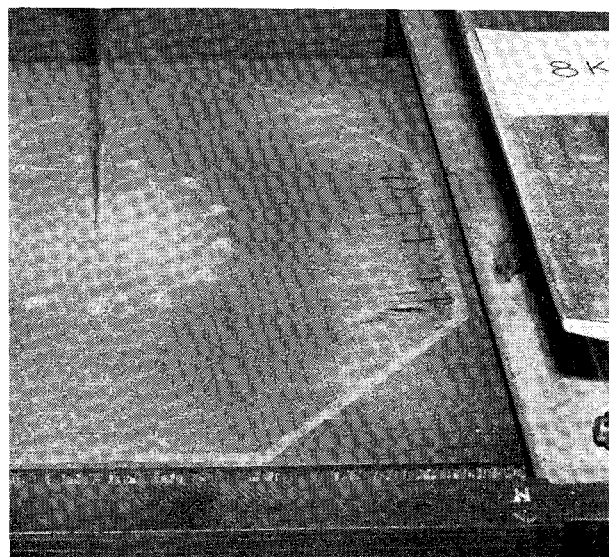


Fig. 18 Incipient failure developing at 35% of parent allowable compression.

19-in. × 60-in. uniformly loaded test panels, was used to test the large scale demonstration components. Five different test panels were constructed representing low- and high-load components, sandwich and plate construction, on aircraft and off, partial damage and through damage in areas to 100 square inches. The program was completed in February 1979.

The work has demonstrated that graphite/epoxy structures, designed in a variety of forms and for a wide range of load intensities, can effectively be repaired to their original strength. Repair concepts have been validated through the required environmental and load condition tests. Repairs in flat panels have been successfully demonstrated. Procedures used have proven to be not only structurally sound, but also relatively easy to implement.

Appendix: Load Transfer Analysis

An elementary analysis based on the assumption that the load in each adherend is proportional to the relative adherend stiffness is found to be entirely satisfactory when applied at each ply of the adherends. While this procedure does not account for shear lag in the adhesive, it does account for the heterogeneous nature of the laminate and gives a satisfactory description of the shear distribution along the entire splice.

The procedure is illustrated in Fig. A1 for a flush scarf joint of identical 16-ply $[(0/\pm 45/90)_2]_s$ laminates. The stiffness distribution on both laminates is given on the small bar chart to the left of the sketch. The values are a function of the laminate ply distribution and the lamina elastic properties. They can be found from the lamina stress SIGX printout of the SQ5 program of Ref. 6. By assigning the thickness per ply the value of unity, the relative Et values of each adherend are determined by accumulating the relative E values at each station as thickness is increased by one ply per station increment. Knowing the (relative) Et of each adherend, the total ET is found and the relative load in one adherend determined from the assumption that the load in each adherend is proportional to the adherend Et .

The difference in the load fraction at two adjacent stations is the average relative shear (RS) loading for the increment, i.e.,

$$(RS)_{i,i-1} = (L/T)_i - (L/T)_{i-1}$$

where

L_i = left Et of station i

T_i = total Et of station i

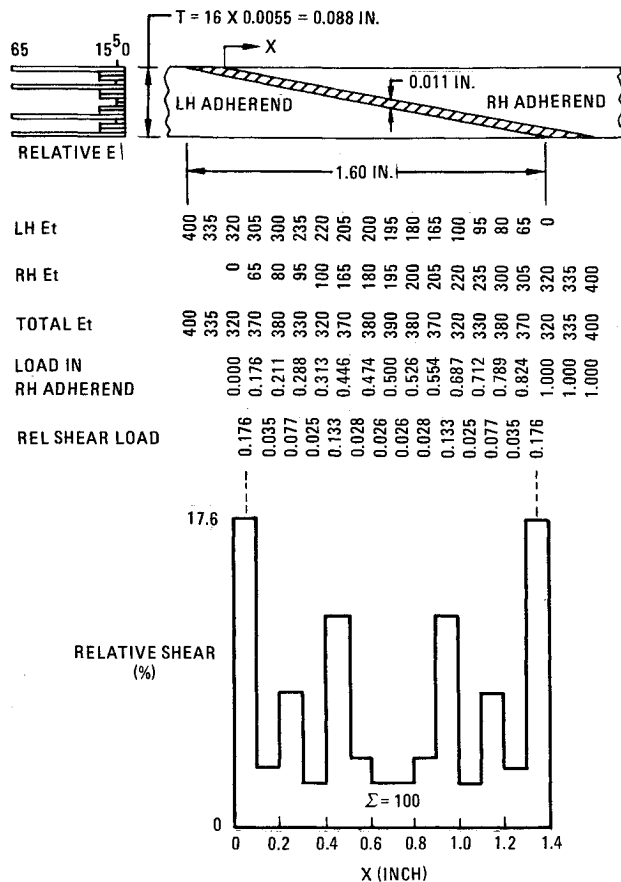


Fig. A1 Shear distribution analysis for scarf-joint with identical $[0/\pm 45/90]_2$ adherends.

The relative shear diagram (Fig. A1) gives some insight into the load-transfer mechanics. No claim is made for precision since shear lag is neglected, but the general nonuniformity is rationally determined. The higher shears exist on those steps where the 0-deg ply of the thinner adherend is bonded.

The strength of the splice is inversely proportional to the maximum relative shear, i.e.,

$$P_{ULT} = F_{SU}(\Delta x) / MRS$$

Fig. A3 Shear distribution analysis with added 0-deg plies.

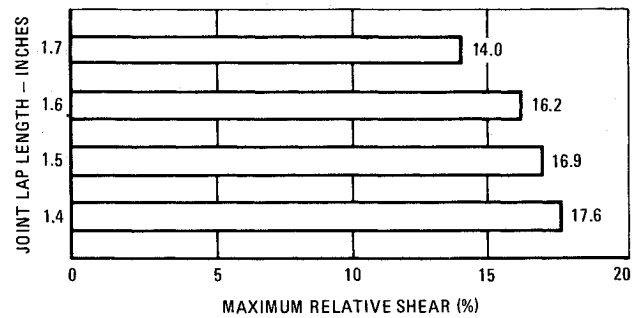
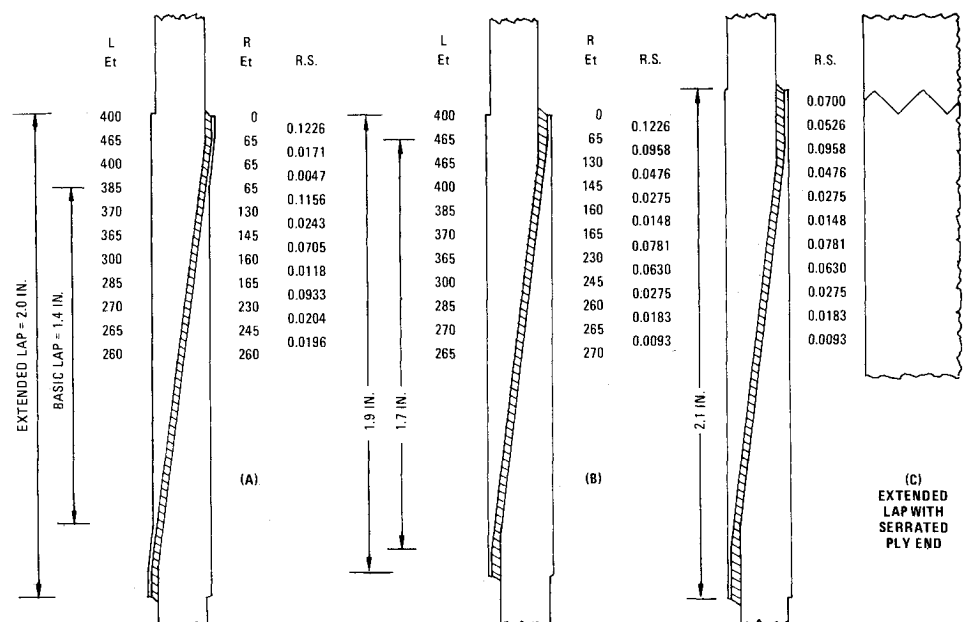


Fig. A2 Effect of lap length on MRS.

where

F_{SU} = adhesive ultimate shear strength, psi

Δx = station increment, in.

MRS = maximum relative shear

Adhesive shear strengths are uniquely related to the kind of test performed. The rub comes in applying such data to design. The joint analysis has roughly determined the shear distribution on the bondline using station increments corresponding to a thickness change of one ply. Shear strength determined by the rail shear test on FM-400 adhesive has been found to relate adequately to this analysis.

The significant design question is, "What can be done to reduce the maximum relative shear?" The intent of this simple analysis is to quickly draw attention to such problem areas. Innovative remedial action is possible if we understand where the problem is.

The scarf joint in Fig. A1 is flush on both surfaces, hence, 0.2 in. shorter than the length of the scarf. Consider the effect of increasing the overlap of the two adherends. The maximum relative shear is reduced as shown in Fig. A2.

Another approach to reducing the maximum relative shear is to add a 0-deg ply on both surfaces over the splice and extending a short distance beyond as shown in Fig. A3a. Both added plies should terminate at the same station. The maximum relative shear of 0.1226 at the end of the added ply results from assuming again a 0.1-in. increment to transfer the load. The next largest relative shear is 0.1156 in Fig. A3a.

If the basic lap is increased to 1.7 in. together with the added plies as in Fig. A3b, the $MRS = 0.1226$ remains unchanged but the next largest relative shear is reduced to 0.0958. To reduce the maximum value, the extended lap length is increased to 2.1 in. and the ends of the added plies serrated as shown in Fig. A3c. Serrating can be done easily with pinking shears. With 0.1-in.-deep serrations and again assuming 0.1 in. to load any fiber, the relative shear at the longest ply end is reduced by nearly half. The maximum relative shear now becomes 0.0958 as seen in Fig. A3c. The precise effect of the serration is beside the point here, if in fact the relative shear at the ply end is reduced below the 0.0958 level, which now defines the shear strength of the splice. Tests have indeed shown that serrating the end of the long plies substantially improves the strength of a splice.

The effect of hot wet conditions should be considered carefully because several changes are effected. The matrix-dominated elastic properties (E_2 and G_{12}) are greatly reduced at 265°F wet conditions. The resulting relative E values for the (0/±45/90) laminate at 265°F wet are (73/13/13/1), respectively (more heterogeneous than for room temperature dry). Shear analysis for the joint of Fig. A3c using these values results in a maximum relative shear of 0.1022. This 7% increase in the MRS weakens the joint in addition to the thermochemical effects reducing the strength of the adhesive.

If a shear flow is to be transferred across the joint, the analysis is similar. The essential difference is that lamina shear stiffnesses must be used rather than extensional stiffnesses. A pair of plies at ±45 are about six times as stiff in

shear as a 0/90-deg pair. The relative G values are arranged in the stacking order and the G_I of each adherend determined. The splice of Fig. A3c analyzed for shear flow resulted in a maximum relative shear in two areas. As before, this fraction of shear flow q is transferred in the increment length Δx . Hence:

$$q_{ULT} = F_{SU}(\Delta x) / MRS$$

Acknowledgments

The results presented are from work sponsored by the Air Force Flight Dynamics Laboratory under Contract F33615-76-3017, Large Area Composite Structure Repair.

References

- ¹"Composite Development Program—Graphite/Epoxy Repair Concepts," MDC AC3715, Vol. 4, McDonnell Aircraft Co., March 1976.
- ²Lubin, G., et al., "Repair Technology for Boron/Epoxy Composites," AFML-TR-71-270, Grumman Aerospace Corp., Feb. 1972.
- ³Scow, A.L., et al., "Large Area Composite Structure Repair," First Interim Report, AFFDL-TR-77-5, Northrop Corp., Jan. 1977.
- ⁴Kiger, R.W. and Myhre, S.H., "Large Area Composite Repair," Second Interim Report, AFFDL-TR-77-121, Northrop Corp., Nov. 1977.
- ⁵Verette, R.M. and Labor, J.D., "Structural Criteria for Advanced Composites," AFFDL-TR-76-142, Vol. 1, Northrop Corp., March 1977.
- ⁶Reed, D.L., "Point Stress Laminate Analysis," Report FZM-5494, General Dynamics/Fort Worth, April 1970.

From the AIAA Progress in Astronautics and Aeronautics Series..

EXPERIMENTAL DIAGNOSTICS IN COMBUSTION OF SOLIDS—v. 63

Edited by Thomas L. Boggs, Naval Weapons Center, and Ben T. Zinn, Georgia Institute of Technology

The present volume was prepared as a sequel to Volume 53, *Experimental Diagnostics in Gas Phase Combustion Systems*, published in 1977. Its objective is similar to that of the gas phase combustion volume, namely, to assemble in one place a set of advanced expository treatments of the newest diagnostic methods that have emerged in recent years in experimental combustion research in heterogeneous systems and to analyze both the potentials and the shortcomings in ways that would suggest directions for future development. The emphasis in the first volume was on homogeneous gas phase systems, usually the subject of idealized laboratory researches; the emphasis in the present volume is on heterogeneous two- or more-phase systems typical of those encountered in practical combustors.

As remarked in the 1977 volume, the particular diagnostic methods selected for presentation were largely undeveloped a decade ago. However, these more powerful methods now make possible a deeper and much more detailed understanding of the complex processes in combustion than we had thought feasible at that time.

Like the previous one, this volume was planned as a means to disseminate the techniques hitherto known only to specialists to the much broader community of research scientists and development engineers in the combustion field. We believe that the articles and the selected references to the current literature contained in the articles will prove useful and stimulating.

339 pp., 6 × 9 illus., including one four-color plate, \$20.00 Mem., \$35.00 List

TO ORDER WRITE: Publications Dept., AIAA, 1290 Avenue of the Americas, New York, N.Y. 10019